

Directional Compton profiles of silver

A. Andrejczuk and L. Dobrzyński

Institute of Physics, Warsaw University Branch in Białystok, Lipowa 41, Poland

J. Kwiatkowska and F. Maniowski

Institute of Nuclear Physics, Cracow, Radzikowskiego 152, Poland

S. Kaprzyk

*Department of Physics, Northeastern University, Boston, Massachusetts 02115
and Academy of Mining and Metallurgy, Cracow, Al. Mickiewicza 30, Poland*

A. Bansil

Department of Physics, Northeastern University, Boston, Massachusetts 02115

E. Żukowski

*Department of Physics, University of Warwick, Coventry CV4 7AL, United Kingdom
and Institute of Physics, Warsaw University Branch in Białystok, Lipowa 41, Poland*

M. J. Cooper

Department of Physics, University of Warwick, Coventry CV4 7AL, United Kingdom

(Received 1 March 1993)

The [100], [110], and [111] directional Compton profiles from Ag single crystals measured using ^{198}Au (412 keV) and ^{137}Cs (662 keV) sources, together with the corresponding theoretical profiles obtained within the charge self-consistent relativistic Korringa-Kohn-Rostoker band-structure methodology are presented. The overall amplitude and shape of the measured directional anisotropies are found to be in good accord with theoretical predictions based on the local-density approximation. In considering absolute Compton profiles, a substantial discrepancy between theory and experiment is found; however, this discrepancy is essentially removed by invoking an energy-independent correction to the data consistent with the presence of a significant bremsstrahlung background. The experimental and theoretical results are compared and contrasted with other relevant available data in the literature.

I. INTRODUCTION

It is well known that Compton profile (CP) measurements can be used to characterize the electronic structure of materials.¹⁻³ The energy spectrum of monoenergetic photons inelastically scattered from electrons in the target is intimately related through the Doppler effect with the electron momentum-density distribution,

$$n(\mathbf{p}) = \sum_i \left| \int \Psi_i(\mathbf{r}) \exp(i\mathbf{p}\cdot\mathbf{r}) d^3r \right|^2, \quad (1)$$

where \mathbf{p} denotes momentum, and $\Psi_i(\mathbf{r})$ are the electron wave functions. The summation in (1) extends over all occupied states. The Compton profile $J(p_z)$ essentially is

$$J(p_z) = \int \int n(\mathbf{p}) dp_x dp_y. \quad (2)$$

The Fourier transform involved in (1) implies that diffuse conduction electrons with broad wave functions will form the low-momentum part of the CP. For this reason, studies of Compton line shapes can, in principle, provide a sensitive test of the validity of the local-density approximation- (LDA) based band-theory predictions.⁴⁻⁹

Numerous Compton scattering studies of light elements have been reported.¹⁻³ However, investigations of heavier elements are less common and often less accurate because the high- Z elements require high-photon energies (in order to overcome the photoabsorption problem), and not many γ -ray sources which possess a single high-energy line are available. In fact, only three such sources are in practical use: ^{51}Cr ($E_\gamma = 320$ keV, $T_{1/2} = 29$ d), ^{198}Au ($E_\gamma = 412$ keV, $T_{1/2} = 2.7$ d), and ^{137}Cs ($E_\gamma = 662$ keV, $T_{1/2} = 30$ yr). ^{51}Cr and ^{198}Au sources are relatively expensive owing to their short lifetime. On the other hand, in the ^{137}Cs source, used first by DuBard,¹⁰ the lower specific activity and the larger associated source volume make it more difficult to model the self-absorption and internal multiple-scattering effects. Despite these inherent difficulties, the CP's of many heavy elements have been studied, including Zr (Ref. 11), Nb (Ref. 12), Rh (Ref. 13), Ag (Refs. 9,14,15), Cd (Ref. 16), W (Ref. 17), Pt and Au (Ref. 18), and a more extensive use of the ^{137}Cs source appears warranted. We note that the momentum resolution possible via line sources is never better than about 0.37 a.u. full width at half maximum (FWHM); significant improvement may be expected with the advent of crystal spectrometers at the high-

brightness synchrotron radiation facilities.¹⁹

Compton profiles along the three low-index directions from a Ag single crystal have been reported recently by Manninen and Paakkari⁹ using a ²⁴¹Am source. We were motivated to undertake the present study, however, for several reasons. First, the momentum resolution in Ref. 9 was worse than that which can be achieved with the ¹³⁷Cs spectrometer. Second, the elastic-scattering peak which presents problems with the 59.54 keV Am source gives practically no contribution either at the 412 keV Au line or the 662 keV Cs line since it is separated from the Compton line by several hundred keV. The Au and Cs sources also possess the advantage that the fluorescent radiation from the sample appears in the low-energy region, once again far from the Compton peak. On the other hand, the treatment of bremsstrahlung radiation associated with photoexcited electrons in the sample,⁹ and the uncertainty concerning the correct form of the Compton scattering cross section,²⁰ may become more serious problems with high-energy sources.

In this paper, we also extend the comparison between theory and experiment to include *absolute* CP in Ag; the work of Manninen and Paakkari⁹ only considered directional anisotropies in the profiles. For this purpose we have carried out extensive calculations of CP's in Ag using the Koringa-Kohn-Rostoker (KKR) band-structure scheme,²¹ and obtained various contributions to the CP's, i.e., the valence, the core, and the Lam-Platzman^{22,23} corrections, within the same consistent framework. Such an approach is more satisfactory, especially when absolute CP's are considered, than the use of different methods for obtaining different parts of the CP, as appears to be the case in much of the existing work comparing theoretical and experimental CP's. Our theoretical results are in good accord with available published work on Ag, especially the nonrelativistic calculations of Fuster *et al.*²⁴ for the valence electron CP based on the linear combination of Gaussian orbital (LCGO) scheme.^{25,26} It may be noted that we have been motivated to develop the KKR methodology for computing CP's because this is the only approach which allows a similar first-principles treatment of the electronic structure and CP's in disordered alloys, which are also of interest to us.²⁷

An outline of this paper is as follows. The introductory remarks are followed in Sec. II with a delineation of the details of sample preparation and other experimental aspects of the measurements. Section III summarizes the relevant aspects of our theoretical calculations. Section IV presents and discusses our experimental and theoretical results, followed in Sec. V by some concluding remarks.

II. EXPERIMENTAL CONSIDERATIONS

A single crystal of Ag (99.999%-purity) was grown by the Bridgman-Stockbarger method. Plane-parallel slices, 2 mm thick, were cut perpendicular to the [100], [110], and [111] crystallographic directions with a wire saw. The disks (about 15 mm diam) so obtained were ground with abrasive papers and chemically etched and electro-

polished, yielding three specimens of nearly identical shapes (14.3 mm diam, 1.5 mm thick disks). A more careful check showed a difference of 0.02 mm (1.5%) in the thickness of the [100] and [111] samples; this difference was taken into account in processing the raw data. The orientation of the samples was checked via Laue diffraction, and all specimens were found to be aligned within 2°.

The samples were glued to a cross made of thin strips of adhesive tape. The beam cross section and the area seen by the detector at the sample position were the same, 177 mm². The samples were oriented with the scattering vector lying along the appropriate face normal with an accuracy better than 1°. Two Au plates 8.0×8.0×0.8 mm³ were irradiated at the Institute of Atomic Energy at Świerk to the activity of around 100 Ci; the ¹³⁷Cs had an activity of 90 Ci. The momentum resolution is estimated to be 0.37 and 0.40 a.u. with the Au and Cs sources, respectively. For each source, 0.29×10⁶ counts/50 eV channel were taken at the peak maximum, giving a total of 7×10⁷ counts under the Compton peak in the range -10 to 10 a.u. This required a measuring time (per sample) of about two weeks with the Cs source, and about one week with the Au source. The background, also measured during a two-week period for the Cs source without the sample, was $\frac{1}{40}$ of the signal; the corresponding background for the Au source was $\frac{1}{130}$.

Some relevant details of our Compton spectrometer are as follows (see Ref. 28 for a more extensive discussion). The scattering is performed in a 170×40×40 cm³ rectangular chamber, the construction allowing the use of either the ¹⁹⁸Au or the ¹³⁷Cs source. For the ¹⁹⁸Au source, the chamber was evacuated to a pressure below 0.1 mbar in order to minimize air scattering. This, however, was not done for the ¹³⁷Cs source since the low pressure could rupture the source capsule. Instead, the chamber was filled with He gas at normal pressure which resulted in an improved signal-to-background ratio by a factor of about 3. In view of the rather long duration of the measurements (a total of about two months for three samples), a continuous flow of pure He was maintained through the chamber, and the purity of He was further monitored via the speed of sound measurements performed on the outgoing gas in a long pipe connected to the chamber. The source to sample, and the sample to detector distances were 422 and 661 mm, respectively; the scattering angle was 166.9±0.6°. A Ge detector (GLP Ortec, 10 mm thick, 16 mm diam) with a TC-244 Tennelec amplifier and a 919-Spectrum Master Ortec multichannel analyzer was used to collect 4096 channels of data. The numerical stabilization of gain during the experiment was achieved by using the position of the Pb K α_1 fluorescent peak, as well as the peak from a ⁵⁷Co calibration source. The spectrum was saved every day and the overall peak shift was found to be less than 0.1 channel.

We have used the Cs source primarily for investigating the electron momentum-density anisotropies by measuring differences between CP's for various crystallographic directions in order to reduce systematic errors. A similar use of the Au source to determine anisotropies⁷ involved

problems due to the short half-life of the source and the presence of an admixture of ^{199}Au which gives an elastic contribution to the Compton peak. Since the half-lives of the two Au isotopes are different, the order of measurements on various samples may become important. Therefore, measurements for two different crystallographic orientations should be repeated in reverse order using sources prepared under identical irradiation conditions. Our experience with Ag samples indicates that such a procedure can, indeed, yield high-quality data despite an increased experimental cost. Bearing these considerations in mind, the Au source was used only in two samples; the Cs measurements were, however, carried out for all three specimens prepared.

In processing the raw experimental data, corrections for the background, the detector response function, the detector efficiency, the sample absorption, and the Compton scattering cross section were made; the details are described elsewhere.^{7,28} For the ^{137}Cs data, it was difficult to model effects of self-absorption and multiple scattering within the source due to a lack of full knowledge of the source composition, as noted above. In order to gain insight into this problem, we reanalyzed our earlier ^{137}Cs data²⁸ on Al and found that the Compton peak asymmetry could be treated satisfactorily by adjusting the low-energy side of the instrumental resolution function (IRF). An increase in the amplitude of the low-energy tail to 0.3% of the maximum of the full energy peak (compared to 0.01% for the Au source) reduced the asymmetry of the profile in Al to within 1.3% of the maximum; this empirical correction to the IRF was also used to deconvolute the present ^{137}Cs data on Ag. The systematic asymmetry for the ^{198}Au data did not exceed 1%, and furthermore, in this case the self-scattering corrections were obtained via Monte Carlo simulations; since all corrections were obtained *ab initio*, the absolute profiles for ^{198}Au should be considered more reliable. The photon multiple-scattering corrections are estimated, via a Monte Carlo procedure, to be 19% and 18% for the Au and Cs data, respectively. The multiple-scattering corrections for the [111] sample which was 1.5% thinner than the other two samples were proportionately reduced by 1.5%.

The experimental profiles have been normalized to the theoretical value (see Sec. III below) of 20.59 electrons in the momentum range 0 to 10 a.u. For obtaining directional differences, however, the profiles were normalized within the range -10 to 10 a.u. to twice this value, i.e., 41.18 electrons. The aforementioned left-right asymmetry (about 1 and 1.4% for the Au and Cs data, respectively) is estimated to give corrections to the difference profiles smaller than the statistical error; the left-right averaging was accordingly used to improve statistical accuracy.

III. THEORETICAL CONSIDERATIONS

Our computations are based on the use of the charge self-consistent KKR band-structure scheme utilizing the muffin-tin approximation to the crystal potential.^{29,30} All electrons were included: the core states were treated relativistically while the valence states were obtained within

the semirelativistic approximation.³¹ The von Barth-Hedin³² local-density approximation to the exchange-correlation potential was used. The band-structure problem was solved to a high degree of self-consistency (energy bands, Fermi energy, and potentials converged to better than 1 meV) for the Ag fcc lattice (lattice constant, $a=7.7218$ a.u.) using $l_{\max}=4$ (maximum angular momentum cutoff), before proceeding with momentum-density computations. Nonrelativistic computations were also carried out in order to check our results against those of Moruzzi, Janak, and Williams³³ who have used a similar KKR scheme; the agreement with Ref. 33 with regard to the bands and potentials was within 1 meV.

In order to calculate the Compton profiles, the momentum density $n(\mathbf{p})$ of Eq. (1) was calculated on a mesh containing $48 \times 1183 \times 2421$ *ab initio* \mathbf{p} points; here 48 denotes the symmetry operations of the cubic point group, 1183 the number of \mathbf{k} points in the irreducible $\frac{1}{48}$ th of the Brillouin zone, and 2421 the number of \mathbf{p} points obtained from each \mathbf{k} point by adding reciprocal-lattice vectors. The two-dimensional integrations involved in the evaluation of the CP [Eq. (2)], were carried out by using the tetrahedral method of Lehmann and Taut.³⁴ This approach can be very efficient since the form (3.20) from Ref. 34 is especially amenable to developing highly vectorized computer codes. The final CP's were computed along the [100], [110], and [111] directions on a 201 point uniformly spaced mesh in q (momentum transfer) over the range 0–20 a.u. Based on a variety of computations using different meshes, we estimate that our calculated CP's are accurate to about 5 parts in 10^4 . The total number of valence electrons under the theoretical CP's are also correct (over the 0–20 a.u. range) to about 1 part in 10^4 (see Ref. 35); the core CP's were evaluated separately over the range 0–200 a.u., which reproduced the normalization of the core wave functions to a roughly similar level of accuracy. Finally, Lam-Platzman corrections²² to the CP's were obtained using the occupation number function for the uniform Fermi gas tabulated by Lundqvist.²³

The question of numerical accuracy in Compton profile computations deserves comment. Because the electron momentum density varies slowly with momentum and possesses breaks at Fermi-surface crossings, great care is necessary in obtaining the two-dimensional integral of Eq. (2). A fine mesh in p space must be used to properly account for Fermi-surface breaks, and the limit of integration must extend to a sufficiently high- p value in order to treat the long-range nature of the integrand. Further, the CP itself must be evaluated up to fairly high-momentum-transfer values (q) in order to correctly obtain the normalization of the theoretical CP. Our experience with Ag has been that in order to obtain numerically reliable CP's, we require ~ 1000 \mathbf{k} points in the irreducible $\frac{1}{48}$ th of the Brillouin zone, and a momentum cutoff in Eq. (2) ~ 11 a.u.³⁶

IV. RESULTS AND DISCUSSION

Our main theoretical and experimental results are summarized in Tables I and II, and may be discussed with reference to Figs. 1–4. Table I and Fig. 1 give insight

into various contributions to the CP's and compare our results with the corresponding data of Fuster *et al.*²⁴ and Biggs.³⁷ Recall that the LCGO computations of Fuster *et al.*²⁴ are nonrelativistic and include only the valence states. Accordingly, our KKR results for valence electrons in Table I are also nonrelativistic, and are seen from Fig. 1 to be in good agreement with the LCGO results for all three symmetry directions.³⁸ Figure 1 shows that the core CP is increased by about 0.05 (electrons/a.u.) from its free atom value via solid-state effects, whereas Lam-Platzman corrections amount to -0.06 (electrons/a.u.) at the peak. The relativistic effects (not shown in Fig. 1)

are of the order of Lam-Platzman corrections. It is clear that a satisfactory evaluation of the absolute CP's requires the computation of valence and core contributions, as well as the Lam-Platzman corrections within a single consistent scheme. In particular, an analysis of the absolute CP obtained by adding Biggs' Hartree-Fock core part to the valence part based on the band-theory framework with a Lam-Platzman correction would likely lead to uncertain results, and in any event this procedure is not strictly justified within the logic of the density-functional formalism.

Table II and Fig. 2 compare the measured and comput-

TABLE I. Comparison of various theoretical Compton profiles in Ag along the [100], [110], and [111] directions, in units of electrons/a.u. All computations are within the nonrelativistic approximation. Columns 2-7 give the valence electron contribution for the KKR and the LCGO (Ref. 24) schemes. Columns 8 and 9 give the core electron contribution for the KKR and the free atom Hartree-Fock calculations of Biggs (Ref. 37). The Lam-Platzman (LP) correction based on the KKR charge density is given in the last column.

p_z (a.u.)	[100]		[110]		[111]		Core		
	LCGO	KKR	LCGO	KKR	LCGO	KKR	KKR	Biggs	LP
1	2	3	4	5	6	7	8	9	10
0.000	3.532	3.553	3.578	3.562	3.500	3.513	4.090	4.038	-0.057
0.050	3.527	3.532	3.564	3.554	3.499	3.502	4.088	4.036	-0.056
0.100	3.512	3.529	3.536	3.521	3.497	3.514	4.084	4.032	-0.056
0.150	3.487	3.496	3.481	3.483	3.500	3.506	4.077	4.026	-0.055
0.200	3.454	3.448	3.432	3.445	3.482	3.474	4.068	4.018	-0.054
0.250	3.414	3.410	3.381	3.380	3.444	3.453	4.055	4.006	-0.053
0.300	3.369	3.366	3.323	3.321	3.387	3.390	4.038	3.990	-0.051
0.350	3.330	3.329	3.255	3.263	3.291	3.300	4.020	3.973	-0.049
0.400	3.255	3.260	3.175	3.189	3.183	3.187	3.998	3.953	-0.047
0.450	3.152	3.152	3.080	3.090	3.068	3.080	3.973	3.929	-0.044
0.500	2.992	2.997	2.969	2.980	2.947	2.953	3.945	3.901	-0.041
0.550	2.847	2.848	2.847	2.857	2.830	2.847	3.914	3.870	-0.037
0.600	2.725	2.726	2.698	2.717	2.725	2.743	3.879	3.837	-0.033
0.650	2.621	2.632	2.594	2.614	2.637	2.652	3.842	3.801	-0.028
0.700	2.553	2.562	2.542	2.553	2.567	2.579	3.802	3.763	-0.024
0.750	2.500	2.507	2.491	2.503	2.514	2.521	3.759	3.722	-0.018
0.800	2.446	2.456	2.442	2.454	2.459	2.467	3.713	3.678	-0.011
0.850	2.389	2.398	2.394	2.408	2.401	2.408	3.663	3.631	-0.002
0.900	2.328	2.341	2.349	2.363	2.339	2.347	3.612	3.582	0.005
0.950	2.264	2.280	2.304	2.319	2.275	2.283	3.558	3.530	0.008
1.000	2.206	2.220	2.258	2.273	2.211	2.221	3.503	3.476	0.008
1.100	2.087	2.101	2.157	2.168	2.089	2.098	3.387	3.364	0.008
1.200	1.968	1.979	2.036	2.040	1.973	1.976	3.267	3.247	0.007
1.300	1.832	1.836	1.887	1.883	1.847	1.847	3.143	3.126	0.006
1.400	1.680	1.680	1.727	1.719	1.715	1.711	3.020	3.003	0.005
1.500	1.551	1.549	1.570	1.564	1.575	1.570	2.897	2.880	0.004
1.600	1.430	1.427	1.417	1.411	1.439	1.436	2.777	2.760	0.004
1.700	1.304	1.301	1.257	1.254	1.311	1.308	2.662	2.647	0.004
1.800	1.179	1.180	1.100	1.106	1.183	1.181	2.552	2.540	0.004
1.900	1.070	1.073	1.009	1.011	1.059	1.060	2.448	2.436	0.004
2.000	0.974	0.980	0.931	0.933	0.947	0.952	2.352	2.338	0.004
2.200	0.770	0.775	0.793	0.795	0.777	0.781	2.179	2.166	0.004
2.400	0.622	0.624	0.651	0.653	0.625	0.627	2.033	2.020	0.005
2.600	0.496	0.496	0.515	0.516	0.499	0.499	1.912	1.898	0.005
2.800	0.395	0.394	0.400	0.400	0.393	0.393	1.811	1.797	0.006
3.000	0.303	0.303	0.290	0.290	0.303	0.304	1.726	1.712	0.006
3.500	0.156	0.158	0.157	0.160	0.155	0.158	1.561	1.543	0.006
4.000	0.080	0.084	0.082	0.085	0.079	0.083	1.425	1.419	0.006
5.000	0.028	0.032	0.027	0.032	0.028	0.032	1.179	1.179	0.003

ed absolute CP's in Ag. The ^{198}Au profile along [100] and [110], and the ^{137}Cs data for all three directions are listed in Table II (including the background correction discussed below), along with the total calculated relativistic KKR (RKKR) CP's. The spherically-averaged CP's are also given; these values are in good accord with the corresponding experimental results listed by Manninen and

Paakkari.⁹

We observe first from Fig. 2 that the theoretical CP's differ substantially from the experimental results obtained via the standard processing steps (see Sec. II above, and Ref. 28) from the raw data, i.e., the points labeled [100]exp-RKKR, etc. The measured $J(0)$ is lower than the theoretical predictions with the missing electrons

TABLE II. A comparison of the total experimental and theoretical directional (columns 2–9) and spherically-averaged (columns 10,11) Compton profiles in Ag, in units of electrons/a.u. The experimental data are listed after all corrections, including the subtraction of background associated with bremsstrahlung from photoelectrons (see text). All three symmetry directions were measured with ^{137}Cs , but for ^{198}Au only the [100] and [110] directions were measured. The experimental error bars vary between $\pm 0.1\%$ at $p_z=0$, increasing to $\pm 0.4\%$ at $p_z=5$ a.u. In the theoretical calculations (RKKR) the valence electrons are treated semirelativistically while the core electrons are treated fully relativistically, and the Lam-Platzman corrections are included. All theoretical profiles have been broadened with a Gaussian of 0.40 a.u. FWHM to reflect the experimental resolution. The spherically-averaged profiles in the last two columns were obtained from the directional profiles via the definition, $J_{\text{sph}} = (6J_{100} + 12J_{110} + 8J_{111})/26$.

p_z (a.u.)	[100]			[110]			[111]		Spherical	
	^{198}Au	^{137}Cs	RKKR	^{198}Au	^{137}Cs	RKKR	^{137}Cs	RKKR	^{137}Cs	RKKR
1	2	3	4	5	6	7	8	9	10	11
0.000	7.495	7.508	7.488	7.501	7.507	7.470	7.510	7.474	7.508	7.475
0.050	7.495	7.511	7.481	7.495	7.505	7.463	7.501	7.468	7.505	7.469
0.100	7.482	7.495	7.462	7.477	7.485	7.443	7.483	7.450	7.487	7.449
0.150	7.456	7.463	7.431	7.446	7.449	7.409	7.454	7.419	7.454	7.417
0.200	7.416	7.416	7.386	7.400	7.399	7.361	7.412	7.374	7.407	7.371
0.250	7.363	7.358	7.327	7.335	7.335	7.300	7.353	7.316	7.345	7.311
0.300	7.297	7.287	7.255	7.257	7.259	7.226	7.279	7.243	7.272	7.238
0.350	7.216	7.204	7.169	7.171	7.176	7.139	7.193	7.156	7.188	7.151
0.400	7.122	7.110	7.070	7.078	7.083	7.042	7.096	7.075	7.093	7.053
0.450	7.015	7.003	6.961	6.979	6.974	6.935	6.992	6.949	6.986	6.945
0.500	6.899	6.888	6.844	6.875	6.858	6.821	6.881	6.834	6.872	6.830
0.550	6.781	6.768	6.722	6.765	6.739	6.703	6.764	6.715	6.754	6.711
0.600	6.659	6.644	6.598	6.650	6.620	6.584	6.644	6.595	6.633	6.591
0.650	6.535	6.515	6.475	6.531	6.502	6.467	6.521	6.476	6.511	6.471
0.700	6.411	6.388	6.355	6.411	6.387	6.353	6.399	6.359	6.391	6.355
0.750	6.289	6.268	6.239	6.294	6.280	6.243	6.281	6.244	6.277	6.242
0.800	6.169	6.153	6.125	6.181	6.174	6.137	6.164	6.131	6.166	6.132
0.850	6.053	6.041	6.013	6.073	6.065	6.034	6.046	6.019	6.054	6.025
0.900	5.940	5.931	5.902	5.967	5.954	5.931	5.930	5.908	5.941	5.917
0.950	5.828	5.820	5.791	5.858	5.838	5.828	5.816	5.795	5.827	5.809
1.000	5.716	5.707	5.677	5.748	5.721	5.722	5.704	5.681	5.713	5.699
1.100	5.484	5.467	5.444	5.521	5.501	5.498	5.480	5.448	5.487	5.470
1.200	5.237	5.224	5.200	5.285	5.262	5.254	5.242	5.208	5.247	5.228
1.300	4.987	4.986	4.949	5.032	5.011	4.993	4.996	4.961	5.001	4.973
1.400	4.740	4.729	4.696	4.765	4.746	4.722	4.742	4.711	4.741	4.712
1.500	4.489	4.470	4.445	4.493	4.474	4.449	4.483	4.459	4.476	4.451
1.600	4.241	4.230	4.201	4.228	4.226	4.182	4.241	4.212	4.232	4.195
1.700	4.000	4.002	3.966	3.976	3.981	3.928	4.007	3.971	3.994	3.950
1.800	3.773	3.782	3.743	3.739	3.739	3.693	3.774	3.740	3.760	3.719
1.900	3.557	3.566	3.532	3.525	3.538	3.484	3.555	3.523	3.550	3.507
2.000	3.351	3.365	3.333	3.327	3.336	3.299	3.354	3.322	3.348	3.314
2.200	2.988	3.005	2.972	2.982	2.996	2.977	3.006	2.968	3.001	2.973
2.400	2.681	2.696	2.667	2.705	2.718	2.691	2.694	2.670	2.706	2.679
2.600	2.433	2.443	2.417	2.445	2.450	2.435	2.446	2.418	2.447	2.426
2.800	2.208	2.229	2.209	2.214	2.236	2.213	2.233	2.209	2.233	2.211
3.000	2.036	2.052	2.036	2.035	2.044	2.028	2.055	2.036	2.049	2.032
3.500	1.719	1.738	1.722	1.719	1.728	1.722	1.736	1.722	1.733	1.722
4.000	1.510	1.518	1.513	1.519	1.525	1.514	1.525	1.512	1.523	1.513
5.000	1.220	1.225	1.215	1.220	1.222	1.215	1.219	1.215	1.222	1.215

spread in the wings of the profiles, all profiles having been normalized to the same area. The discrepancy is seen to be different for the two sources, the largest value being about -0.3 electrons/a.u. or -0.45 electrons/a.u. for zero-momentum transfer ($q=0$), for the ^{198}Au and ^{137}Cs , respectively. The presence of an additional background in the experiment is suggested. We believe this background is related to the bremsstrahlung radiation from photoelectrons excited in the sample; this background would be omitted from measurements made by removing the sample from the scattering chamber.³⁹

The aforementioned bremsstrahlung background warrants further comment. Two contributions are important in this connection. The first comes from outer electrons ejected in Compton scattering with energy gains of ≈ 260 keV for ^{198}Au and ≈ 480 keV for the ^{137}Cs source. The second contribution arises from electrons ejected in the photoabsorption process from the lower shells (e.g., the K shell with binding energy ≈ 25 keV) which gain an energy of ≈ 380 and ≈ 630 keV for the ^{198}Au and ^{137}Cs sources, respectively. These ejected photoelectrons can yield a broad bremsstrahlung spectrum under the Compton line which extends over 138–182 keV for ^{198}Au and over 158–214 keV for the ^{137}Cs case; the fluorescence which may also appear in these processes lies at a much lower energy and is not important, as already noted. Further,

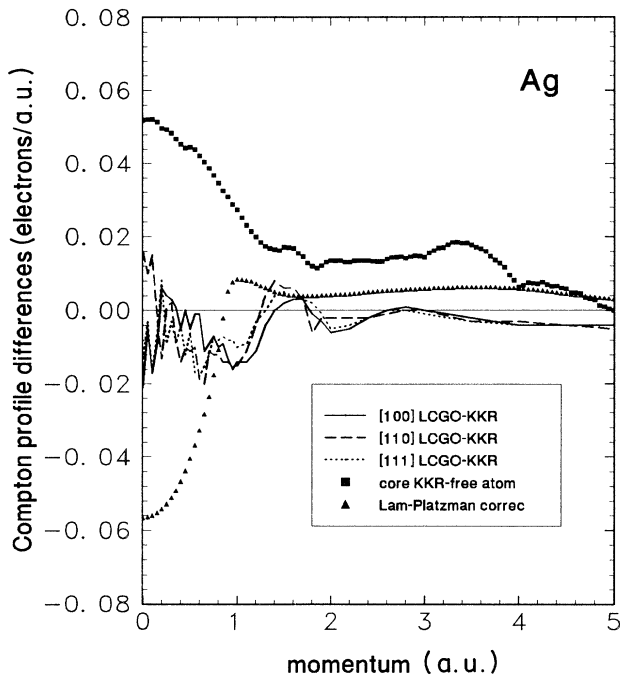


FIG. 1. Differences between various calculated Compton profiles given in Table I are displayed graphically. For example, the solid line gives a plot of the difference between columns 2 and 3 of Table I (see legend for the meaning of other points). Filled squares give the difference between the KKR and free atom core part (Ref. 37) (columns 8 and 9, Table I). The Lam-Platzman correction term (column 10, Table I) is shown by filled triangles.

since the bremsstrahlung cross section is proportional to Z^2 , this contribution will increase with electron as well as photon energies, making this an important effect in this study, even though this effect was negligible in the work of Ref. 9.

Electrons of energy ~ 500 keV possess a range of ~ 0.2 mm in Ag. Since our samples were 1.5 mm thick, most photoelectrons will be stopped in the sample, i.e., the so-called thick absorber case is appropriate (see Chap. 21 in Ref. 39). The bremsstrahlung spectrum is difficult to model precisely in this case because, contrary to the case of photoelectrons of a specific energy, the energies of the photoelectrons in the Compton process vary depending upon the scattering angle, the expected energy range be-

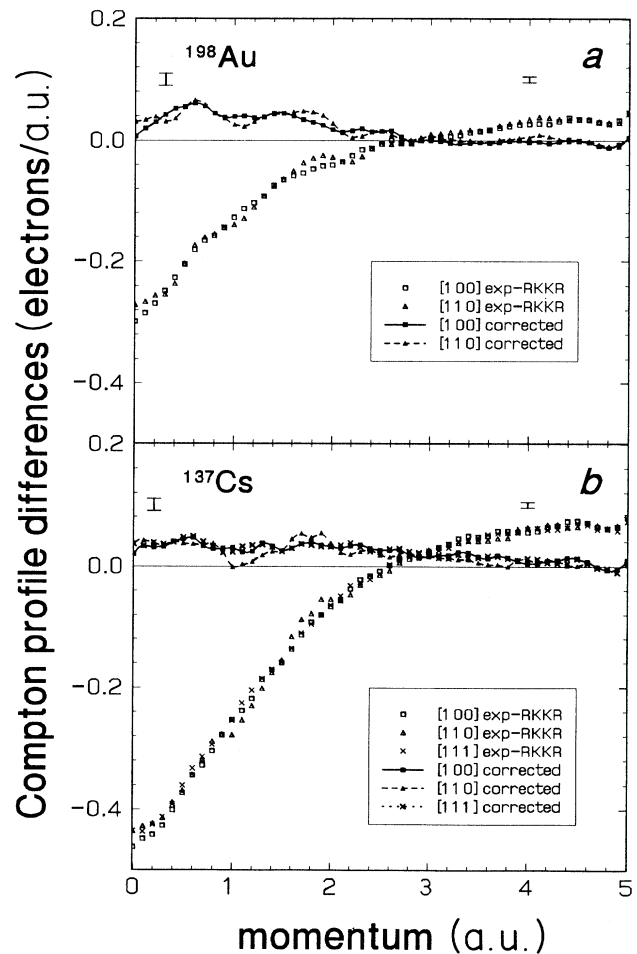


FIG. 2. Differences between the theoretical and experimental absolute directional Compton profiles of Ag for (a) the ^{198}Au and (b) the ^{137}Cs source. The theoretical data here are the same as that given in Table II (columns marked RKKR). The corrected experimental data (see legend) also are the same as in Table II, and include the bremsstrahlung background correction (filled squares, filled triangles, and crosses joined by various lines). The differences between theory and experiment if the bremsstrahlung correction is not made are seen to be quite substantial (open squares, open triangles, and crosses, not joined by lines). Statistical error bars are shown above two points.

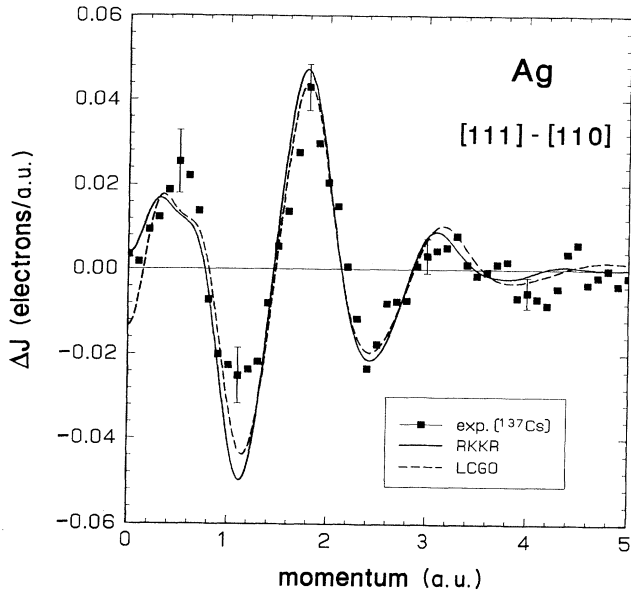


FIG. 3. A comparison of the experimental and theoretical [111]-[110] difference Compton profile ΔJ in Ag. The experimental points (filled squares) are for ^{137}Cs obtained from the data in Table II, and include the bremsstrahlung background correction; typical error bars are shown. The theoretical results (RKKR), solid line) are also based on Table II; the LCGO results (Ref. 24) are based on the valence electron contribution given in Table I, except it is broadened with a Gaussian of 0.4 a.u. FWHM to reflect the experimental resolution.

ing 0–260 keV for ^{198}Au and 0–480 keV for the ^{137}Cs source. Therefore, the bremsstrahlung energy dependence discussed by Manninen and Paakkari [see Eq. (1) of Ref. 9] is simply not applicable in our case.

However, the fact that our measured CP only exhibits

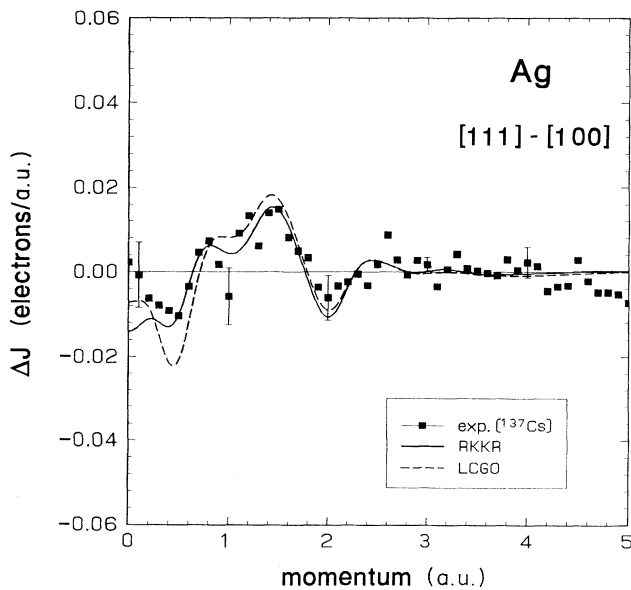


FIG. 4. Same as the caption to Fig. 3, except that this figure refers to the difference profile [111]-[100].

a small left-right asymmetry indicates that the additional background cannot possess a substantial energy dependence in the region of the Compton peak. If so, it is reasonable to model this additional background (bremsstrahlung contribution) by a constant term; with this motivation, we have obtained corrected CP's using the size of this constant as a single adjustable parameter to fit theory. The experimental values after such a correction is applied, listed in Table II, are seen from Fig. 2 to show a dramatic improvement in the agreement between theory and experiment. The background intensities estimated empirically in this manner (over the momentum range -10 to 10 a.u.) are about 5 and 10 % of the Compton intensities for ^{198}Au and ^{137}Cs , respectively. The maximum differences in $J(q)$ of order 0.04 electrons/a.u. seen for the corrected data are comparable to the best level of accord with band theory achieved previously in *d*-band metals such as Ni (Ref. 7), and only somewhat worse than in *s-p* electron metals such as Be.⁵ Although further experimental and theoretical work is warranted in order to precisely determine the bremsstrahlung intensity in CP's of heavy elements with high-energy photons, the results of Fig. 2 suggest that the LDA-based band-theory framework could provide a reasonable description of the absolute Compton spectra of Ag; the discrepancies of order 0.04 electrons/a.u. are probably inherent in such comparisons as differences of this level are present in different band-structure computations (see Fig. 1).

Figures 3 and 4 consider anisotropies in CP's via differences along pairs of directional profiles; the [110]-[100] spectrum is not shown for brevity reasons as it follows simply by taking the difference of the spectra of Figs. 3 and 4. The results for ^{137}Cs are shown, since as noted above the anisotropic profiles for ^{137}Cs are more reliable than for the ^{198}Au source.⁴⁰ The overall agreement between theory and experiment is seen to be excellent with respect to not only the shape but also the amplitude of the anisotropies, although some discrepancies are present. For example, in the [111]-[110] data (Fig. 3) the theoretical dip around 1 a.u. and the peak around 0.05 a.u. lie outside the error bars. However, generally the discrepancies are of the order of differences between the two sets of theoretical results, and cannot be considered serious in view of the size of the error bars on the experimental points and uncertainties in processing the raw data. In contrast, in Ref. 9, the differences between theory and experiment for anisotropies appear more serious for momenta larger than 2 a.u. (Ref. 9 does not consider absolute profiles). For example, the [111]-[110] experimental spectrum of Ref. 9 shows zero crossings around 2.5 and 3.5 a.u. with a negative excursion at intermediate momenta, while Fig. 3 shows a dip around 2.5 a.u. and a zero crossing around 3 a.u.

It may be noted that the aforementioned bremsstrahlung correction does not affect the shape of the directional anisotropies of Figs. 3 and 4 substantially; the data are, of course, to be rescaled appropriately. This is also true of the relativistic effects included in our computations. The core part as well as the Lam-Platzman correction are isotropic and their detailed shape, therefore, does not affect the computed anisotropies.

V. CONCLUSIONS

The directional Compton profiles from Ag single crystals for three high-symmetry directions ([100], [110], and [111]) using two different high-energy sources (^{198}Au and ^{137}Cs) are presented, together with corresponding first-principles all-electron self-consistent calculations within the band-theory framework using the relativistic KKR scheme. A good overall level of agreement between theory and experiment is found with respect to both the shape and amplitude of directional anisotropies. Our study indicates that the anisotropies in Compton spectra of Ag are described quite well by the conventional local-density approximation-based-band-theory framework. We also discuss *absolute* Compton profiles where the band-theory predictions are found to be in substantial disagreement with measurements in Ag. We show, however, that this discrepancy between theory and experiment can be essentially removed by invoking an energy-

independent correction consistent with the presence of a significant bremsstrahlung background radiation associated with photoelectrons excited in the sample; this contribution is not accounted for in background measurements taken by removing the sample.

ACKNOWLEDGMENTS

We are indebted to S. Manninen, D. N. Timms, and B. L. Ahuja for valuable comments. One of us (E.Z.) thanks the SERC and the University of Warwick for financial support. This work was supported by Grant Nos. 2-2350-91-02 and 2-0182-91-01 of the Council of Science Research in Poland, the U.S. DOE under Contract No. W-31-109-ENG-38, including a subcontract to Northeastern University, a travel grant from NATO, and benefited from the allocation of supercomputer time at NERSC, and the Pittsburgh Supercomputer Center.

¹B. G. Williams, *Compton Scattering* (McGraw-Hill, New York, 1977).

²M. J. Cooper, *Rep. Prog. Phys.* **48**, 415 (1985).

³L. Dobrzyński, *Z. Naturforsch. Teil A* **48**, 266 (1993).

⁴Many such studies have been undertaken in various materials; for example, Be (Ref. 5), V (Ref. 6), Cr (Ref. 7), Ni (Ref. 7), Cu (Ref. 8), or Ag (Ref. 9).

⁵P. Rennert, *Phys. Status Solidi B* **105**, 567 (1981); M. Y. Chou, P. K. Lam, and M. L. Cohen, *Phys. Rev. B* **28**, 1696 (1983).

⁶N. Shiotani, Y. Tanaka, Y. Sakurai, N. Sakai, M. Ito, F. Itoh, T. Iwazumi, and H. Kawata, *J. Phys. Soc. Jpn.* (to be published); V. Sundararajan, D. G. Kanhere, and R. M. Singru, *Phys. Rev. B* **46**, 7857 (1992).

⁷A. J. Rollanson, J. R. Schneider, D. S. Laundry, R. S. Holt, and M. J. Cooper, *J. Phys. F* **17**, 1105 (1987); D. A. Cardwell, M. J. Cooper, and S. Wakoh, *J. Phys. Condens. Matter* **1**, 541 (1989); D. A. Cardwell and M. J. Cooper, *ibid.* **1**, 9357 (1989).

⁸P. Pattison, N. K. Hansen, and J. R. Schneider, *Z. Phys. B* **46**, 285 (1982); E. W. Bauer and J. R. Schneider, *ibid.* **54**, 17 (1983); *Phys. Rev. Lett.* **52**, 2061 (1984); *Phys. Rev. B* **31**, 681 (1985).

⁹S. Manninen and T. Paakkari, *Phys. Rev. B* **44**, 2928 (1991).

¹⁰J. L. Du Bard, *Philos. Mag.* **37**, 273 (1978).

¹¹B. K. Sharma and B. L. Ahuja, *Phys. Rev. B* **38**, 3148 (1988).

¹²M. Tomak, H. Singh, B. K. Sharma, and S. Manninen, *Phys. Status Solidi B* **127**, 221 (1985).

¹³F. M. Mohammad, B. K. Sharma, H. Singh, and B. L. Ahuja, *Phys. Status Solidi B* **152**, 145 (1989).

¹⁴B. K. Sharma, H. Singh, S. Perkkiö, T. Paakkari, and K. Manshikka, *Phys. Status Solidi B* **141**, 177 (1987).

¹⁵C.-N. Chang, S.-B. Lee, and C.-C. Chen, *J. Phys. Soc. Jpn.* **60**, 4253 (1991).

¹⁶S. Perkkiö, B. K. Sharma, S. Manninen, T. Paakkari, and B. L. Ahuja, *Phys. Status Solidi B* **169**, 657 (1991).

¹⁷U. Mittal, B. K. Sharma, F. M. Mohammad, and B. L. Ahuja, *Phys. Rev. B* **38**, 12 208 (1988).

¹⁸U. Mittal, S. Perkkiö, B. K. Sharma, S. Manninen, and T. Paakkari, in *Positron Annihilation and Compton Scattering*, edited by B. K. Sharma, P. C. Jain, and R. M. Singru (Omega Scientific, New Delhi, 1990), p. 266.

¹⁹Y. Sakurai, M. Ito, T. Urai, Y. Tanaka, N. Sakai, T. Iwazumi, H. Kawata, M. Ando, and N. Shiotani, *Rev. Sci. Instrum.* **63**, 1190 (1992).

²⁰P. Holm, *Phys. Rev. A* **37**, 3706 (1988).

²¹A. Bansil, *Z. Naturforsch. Teil A* **48**, 165 (1993); P. E. Mijnders and L. P. L. M. Rabou, *J. Phys. F* **16**, 483 (1986); P. E. Mijnders and A. Bansil, *J. Phys. Condens. Matter* **2**, 911 (1990).

²²L. Lam and P. M. Platzman, *Phys. Rev. B* **9**, 5122 (1974).

²³B. I. Lundqvist, *Phys. Kondens. Mater.* **7**, 117 (1968).

²⁴G. Fuster, J. M. Tyler, N. E. Brener, J. Callaway, and D. Bagayoko, *Phys. Rev. B* **42**, 7322 (1990).

²⁵Augmented plane wave results for the valence electron CP in Ag are reported in Ref. 26.

²⁶N. I. Papanicolaou, N. C. Bacalis, and D. A. Papaconstantopoulos, *Handbook of Calculated Electron Momentum Distributions, Compton Profiles, and X-ray Form Factors of Elemental Solids* (CRC, Boca Raton, 1991).

²⁷A. Bansil, in *Electronic Band Structure and its Applications*, edited by M. Yussouff, *Lecture Notes in Physics*, Vol. 283 (Springer, Verlag, Heidelberg, 1987), p. 273; A. Bansil, S. Kaprzyk, and J. Tobola, *Applications of Multiple Scattering Theory to Materials Science*, edited by W. H. Butler, P. H. Dederichs, A. Gonis, and R. L. Weaver, *MRS Symposia Proceedings No. 253* (Materials Research Society, Pittsburgh, 1992), p. 505; A. Bansil, R. S. Rao, P. E. Mijnders, and L. Schwartz, *Phys. Rev. B* **23**, 3608 (1981).

²⁸A. Andrejczuk, E. Żukowski, L. Dobrzyński, and M. J. Cooper (unpublished).

²⁹S. Kaprzyk and A. Bansil, *Phys. Rev. B* **42**, 7358 (1990).

³⁰A. Bansil and S. Kaprzyk, *Phys. Rev. B* **43**, 10 335 (1991).

³¹D. D. Koelling and B. N. Harmon, *J. Phys. C* **10**, 3107 (1977).

³²U. von Barth and L. Hedin, *J. Phys. C* **5**, 1629 (1972).

³³V. L. Moruzzi, J. F. Janak, and A. R. Williams, *Calculated Electronic Properties of Metals* (Pergamon, New York, 1978).

³⁴G. Lehmann and M. Taut, *Phys. Status Solidi B* **54**, 469 (1972).

³⁵In practice, we used an appropriately fitted exponential form for the valence electron CP beyond about 11 a.u. The accuracy of this procedure was, however, checked via *ab initio* com-

putations.

³⁶The augmented plane wave computations of valence electron contribution to the CP of Ref. 26 on Ag are based on 89 k points, and appear to extend to about $p=8$ a.u. A detailed comparison between the data of Ref. 26 and the present computations [or those of Fuster *et al.* (Ref. 24) which closely agree with our results] indicates differences of about 0.13 electron/a.u. in the absolute CP at $q=0$. The anisotropies also possess differences; for example, the [111]-[110] directional anisotropy of Ref. 26 possesses a dip around 1.1 a.u. which is about 50% deeper than that shown in Fig. 3.

³⁷F. Biggs, L. B. Mendelsohn, and J. B. Mann, *Atomic Data and Nucl. Data Tables* **16**, 201 (1975).

³⁸Incidentally, these results suggest that the muffin-tin form of the potential implicit in our approach (as opposed to the use of full potential in LCGO work) yields quite small effects on the CP.

³⁹R. Evans, *The Atomic Nucleus* (McGraw-Hill, New York, 1955), Chap. 20.

⁴⁰In any event, the anisotropic profile [110]-[100] obtained from ¹³⁷Cs and ¹⁹⁸Au is quite similar.